Pion production and absorption in heavy-ion collisions

Yuan Gao,[1,2,*] Yu-Lin Guo,[1] Lei Zhang,[1] Gao-Chan Yong,[2,3] Zi-Yu Liu,[4] and Wei Zuo[2,3]
[1]*School of Information Engineering, Hangzhou Dianzi University, Hangzhou 310018, China*
[2]*Institute of Modern Physics, Chinese Academy of Sciences, Lanzhou 730000, China*
[3]*School of Nuclear Science and Technology, University of Chinese Academy of Sciences, Beijing, 100049, China*
[4]*College of Physics and Electronic Engineering, Xianyang Normal University, Xianyang 712000, China*

(Received 4 May 2021; revised 10 September 2021; accepted 28 September 2021; published 8 October 2021)

Based on the isospin-dependent Boltzmann-Uehling-Uhlenbeck (IBUU) transport model, pion production and absorption are thoroughly studied in the central collision of Au + Au at a beam energy of 400 MeV/nucleon. It is found that the pions are first produced by hard Δ decay at an average density around $1.75\rho_0$, while about 18% of them are absorbed absolutely in the subsequent inelastic collisions. For the free pions observed, more than half of them have been scattered one or more times before they are free from matter, and the higher the scattering numbers of pions, the higher the kinetic energies they possess. These pions, due to longer time of their existence in high density nuclear matter, carry more information about the symmetry energy of nuclear matter at high densities. Moreover, the azimuth dependence and the kinetic energy dependence of the scattering processes and the effect of the symmetry energy are also investigated.

DOI: 10.1103/PhysRevC.104.044607

I. INTRODUCTION

Heavy-ion collisions (HIC) offer a unique possibility to study bulk properties of hot and compressed nuclear matter. One of the main goals of such study is to determine the density dependence of the symmetry energy (SE) at high densities [1–3]. The symmetry energy plays essential roles in understanding a number of physical phenomena and processes. However, it cannot be directly measured in experiments and has to be extracted from observables which are sensitive to the symmetry energy [4].

Pion production is a dominant feature in heavy-ion collisions at intermediate energies [5–9]. In collisions near the pion-production threshold, nuclear matter can be compressed up to about two times normal density ρ_0 before it expands again. During the compression stage the pions are produced mainly from the decay of the Δ resonances created [10–12]. Therefore the pion production is considered to be important for extracting information on the properties of nuclear matter at high densities [13–15]. Since the charged pion ratio in heavy-ion collisions was first suggested in Ref. [16], pion production has attracted much attention in pinning down the density dependence of the symmetry energy. During the last decade, a lot of pionic observables have been proposed as promising probes, such as collective pion flows [17–19], the cone-azimuthal emission of charged pions [20], etc. However, comparing the theoretical results of the π^-/π^+ ratio with the experimental data, analyses came to rather conflicting conclusions on the stiffness of the nuclear symmetry energy at high densities [21–23].

In reactions near the threshold of pion-production the pions are mainly the decay products of the Δ resonances. However, most of them can be absorbed into Δ resonances because of inelastic πN collisions, and then may decay into pions frequently; i.e., the scattering process [24–27]. The details of the scattering process play an important role for extracting information on the symmetry energy at different densities. At the same time, it is commonly known that pions observed are produced at high densities in heavy-ion collisions. The quantitative study of the density at which a pion is produced, as well as the pion's absorption or its scattering, is seldom reported. To further extract information on compressed matter by pionic observables, it is necessary to perform a detailed analysis of the pion production and absorption in HIC.

However, information on the pion's absorption or its scattering process cannot be extracted in experiments so far but can be obtained in theoretical calculations [28,29]. In this paper, a detailed statistical investigation of all the inelastic collisions in the reaction of Au+Au at 400 MeV/nucleon beam energy is performed. All the inelastic collisions are recorded and investigated statistically. Furthermore, the charged pions at freeze-out are categorized by their production and re-scattering processes. The analysis shows the pions are indeed produced at high densities. Moreover about 60% of the pions observed have reabsorption and redecay processes after they were produced the first time, and, due to longer time of their existence in high density nuclear matter, they carry more substantial information on the high-density behavior of the symmetry energy than those without any scattering process, which are produced from hard Δ decay directly and free from matter immediately.

II. THE THEORETICAL MODEL

In the past decade the isospin-dependent Boltzmann-Uehling- Uhlenbeck (IBUU) transport model has been very

*gaoyuan@impcas.ac.cn

successful in describing the dynamical evolution of nucleons in phase space, as well as the reaction dynamics of heavy-ion collisions [30–33]. The present IBUU transport model originating from the IBUU04 model can describe the time evolution of the single-particle phase-space distribution function,

$$\frac{\partial f}{\partial t} + \nabla_{\vec{p}} E - \nabla_{\vec{R}} f = I_c, \tag{1}$$

where I_c is the collision item and $f(\vec{r}, \vec{p}, t)$ is the phase-space distribution function which denotes the probability of finding a particle at time t with momentum $\vec{p}$ at position $\vec{r}$. E denotes the total energy, i.e,, $E = E_{\rm kin} + U$. U is the mean-field potential of the single particle and can be expressed as [34]

$$\begin{aligned} U(\rho, \delta, \mathbf{p}, \tau) = {} & A_u(x)\frac{\rho_{\tau'}}{\rho_0} + A_l(x)\frac{\rho_\tau}{\rho_0} \\ & + B\left(\frac{\rho}{\rho_0}\right)^\sigma (1 - x\delta^2) - 8x\tau\frac{B}{\sigma+1}\frac{\rho^{\sigma-1}}{\rho_0^\sigma}\delta\rho_{\tau'} \\ & + \frac{2C_{\tau,\tau}}{\rho_0}\int d^3\mathbf{p}'\frac{f_\tau(\mathbf{r}, \mathbf{p}')}{1 + (\mathbf{p} - \mathbf{p}')^2/\Lambda^2} \\ & + \frac{2C_{\tau,\tau'}}{\rho_0}\int d^3\mathbf{p}'\frac{f_{\tau'}(\mathbf{r}, \mathbf{p}')}{1 + (\mathbf{p} - \mathbf{p}')^2/\Lambda^2}, \end{aligned} \tag{2}$$

where $\tau, \tau' = \pm 1/2$ denote the neutron and the proton, respectively. The variable x denotes the stiffness of the symmetry energy. Varying the x, one can get different forms of the symmetry energy predicted by various many-body theories without changing any property of symmetric nuclear matter and the value of symmetry energy at normal density ρ_0. The parameters $A_u(x)$, $A_l(x)$ are x dependent and defined as

$$A_u(x) = -95.98 - \frac{2B}{\sigma+1}x, \tag{3}$$

$$A_l(x) = -120.57 + \frac{2B}{\sigma+1}x. \tag{4}$$

The parameter values are $B = 106.35$ MeV and $\sigma = 4/3$. $\Lambda = p_F^0$ is the nucleon Fermi momentum in symmetric nuclear matter, $C_{\tau,\tau'} = -103.4$ MeV, and $C_{\tau,\tau} = -11.7$ MeV. The $C_{\tau,\tau'}$ and $C_{\tau,\tau}$ terms are the momentum-dependent interactions of a nucleon with unlike and like nucleons in the surrounding nuclear matter. With this potential we can get binding energy -16 MeV and incompressibility 211 MeV for symmetric nuclear matter and the symmetry energy 31.5 MeV at saturation density. The resonance Δ potential is given by

$$\begin{aligned} U^{\Delta^-} &= U_n, \\ U^{\Delta^0} &= \tfrac{2}{3}U_n + \tfrac{1}{3}U_p, \\ U^{\Delta^+} &= \tfrac{1}{3}U_n + \tfrac{2}{3}U_p, \\ U^{\Delta^{++}} &= U_p. \end{aligned} \tag{5}$$

In the present work, pions are produced via the decay of Δ resonance [35]. Near the pion-production threshold, the inelastic reaction channels as follows are taken into account [36]:

$$\begin{aligned} NN &\to N\Delta \text{ (hard } \Delta \text{ production)}, \\ N\Delta &\to NN \text{ (}\Delta \text{ absorption)}, \\ \Delta &\to N\pi \text{ (}\Delta \text{ decay)}, \\ N\pi &\to \Delta \text{ (soft } \Delta \text{ production)}. \end{aligned} \tag{6}$$

The free inelastic isospin decomposition cross sections are

$$\begin{aligned} \sigma^{pp\to n\Delta^{++}} &= \sigma^{nn\to p\Delta^-} = \sigma_{10} + \tfrac{1}{2}\sigma_{11}, \\ \sigma^{pp\to p\Delta^+} &= \sigma^{nn\to n\Delta^0} = \tfrac{3}{2}\sigma_{11}, \\ \sigma^{np\to p\Delta^0} &= \sigma^{np\to n\Delta^+} = \tfrac{1}{2}\sigma_{11} + \tfrac{1}{4}\sigma_{10} \end{aligned} \tag{7}$$

The $\sigma_{II'}$ can be parametrized by

$$\sigma_{II'}(\sqrt{s}) = \frac{\pi(\hbar c)^2}{2p^2}\alpha\left(\frac{p_r}{p_0}\right)^\beta \frac{m_0^2\Gamma^2(q/q_0)^3}{\left(s^* - m_0^2\right)^2 + m_0^2\Gamma^2}. \tag{8}$$

Here the I and I' are the initial state and final state isospins of two nucleons; for explicit details and parameters, see Ref. [37]. The cross section for the two-body free inverse reaction can be described by the modified detailed balance,

$$\sigma_{N\Delta\to NN} = \frac{m_\Delta p_f^2 \sigma_{NN\to N\Delta}}{2(1+\delta)p_i^2} \Big/ \int_{m_\pi+m_N}^{\sqrt{s}-m_N} \frac{dm_\Delta}{2\pi} P(m_\Delta), \tag{9}$$

where p_f and p_i are the nucleon center-of-mass momenta in the NN and $N\Delta$ channels, respectively. $P(m_\Delta)$ is the mass function of the Δ produced in NN collision and can be defined according to a modified Breit-Wigner function [38],

$$P(m_\Delta) = \frac{p_f m_\Delta \times 4m_{\Delta 0}^2\Gamma_\Delta}{\left(m_\Delta^2 - m_{\Delta 0}^2\right)^2 + m_{\Delta 0}^2\Gamma_\Delta^2}. \tag{10}$$

Here $m_{\Delta 0}$ denotes the centroid of the resonance and Γ_Δ is the width of the resonance Δ. Assuming that the Δ are produced isotropically in the nucleon-nucleon center of mass, and that the decay of $\Delta \to \pi N$ occurs with an isotropic angular distribution in the Δ rest frame, the width of Δ resonance can be given in a simplistic fashion [39]:

$$\Gamma_\Delta = \frac{0.47q^3}{m_\pi^2[1 + 0.6(q/m_\pi)^2]}. \tag{11}$$

The q is the pion momentum in the Δ rest frame and is defined as

$$q = \sqrt{\left(\frac{m_\Delta^2 - m_n^2 + m_\pi^2}{2m_\Delta}\right)^2 - m_\pi^2}. \tag{12}$$

The decay of the resonance into the nucleon and the pion is carried out by the Monte Carlo method for each time step dt in our calculation, with the probability

$$P_{\rm deacy} = 1 - \exp(-dt\Gamma_\Delta/\hbar). \tag{13}$$

The meson-baryon interactions in our calculations are treated via the formation of baryon resonances, and the Breit-Wigner form of resonance formation can be modified as [40]

$$\sigma_{\pi+N} = \sigma_{\rm max}\left(\frac{q_0}{q}\right)^2 \frac{\frac{1}{4}\Gamma_\Delta^2}{(m_\Delta - m_{\Delta 0})^2 + \frac{1}{4}\Gamma_\Delta^2}, \tag{14}$$

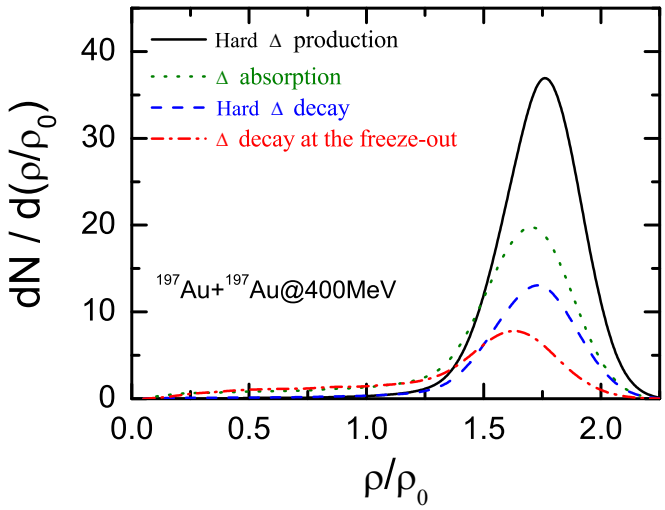

FIG. 1. Local density distributions of the number of different inelastic reactions in the central collision of Au + Au at a beam energy of 400 MeV/nucleon.

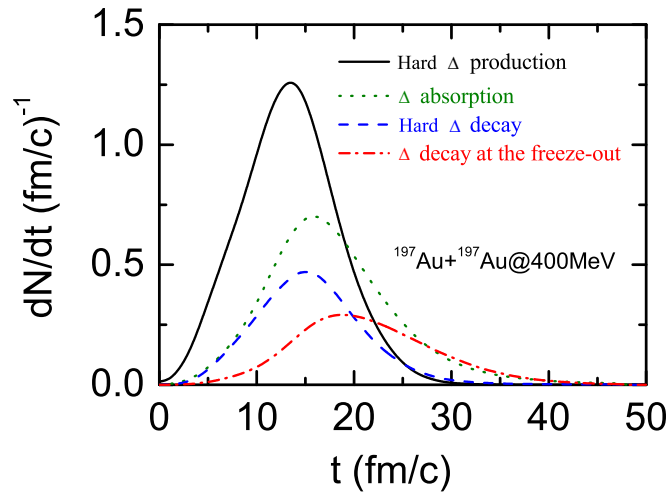

FIG. 2. Time evolutions of the number of different inelastic reactions in the central collision of Au + Au at a beam energy of 400 MeV/nucleon.

where q_0 represents the pion momentum at the centroid $m_{\Delta 0} = 1.232$ GeV of the resonance mass distribution. The maximum cross sections are given by [39,41,42]

$$\begin{aligned} \sigma_{\max}^{\pi^+ p\to\Delta^{++}} &= \sigma_{\max}^{\pi^- n\to\Delta^-} = 200 \text{ mb}, \\ \sigma_{\max}^{\pi^- p\to\Delta^0} &= \sigma_{\max}^{\pi^+ n\to\Delta^+} = 66.67 \text{ mb}, \\ \sigma_{\max}^{\pi^0 p\to\Delta^+} &= \sigma_{\max}^{\pi^0 n\to\Delta^0} = 133.33 \text{ mb}. \end{aligned} \tag{15}$$

III. RESULTS AND DISCUSSIONS

Transport theories have been very successful in describing the reaction dynamics of heavy-ion collisions [28,43–46]. Due to their strong interactions with the nuclear environment, pionic observables at freeze-out are the result of complex creation and rescattering processes. In order to obtain detailed information on the pion's production and its absorption, we study all the inelastic collisions in the central collision of Au + Au at a beam energy of 400 MeV/nucleon within the framework of the IBUU model. First we investigate the numbers of different inelastic reactions and the densities at which they take place, which are shown in Fig. 1. By comparing the solid line and the dashed line, it can be seen that only 40% of hard Δ can decay into pions and the remaining 60% of them are subsequently absorbed into nucleons without any decay. Furthermore, due to the low production threshold, pions are reabsorbed and reproduced quite frequently. About 18% of the pions from hard Δ will be absorbed thoroughly, and the rest will be free particles ultimately, but probably having one or more scattering processes ($\pi N \to \Delta \to \pi N$) before they are detected.

In Fig. 1 we can also see that the reaction $NN \to N\Delta$ takes place at an average density around $1.75\rho_0$, and, in almost same range of density, the hard Δ decay into pions. Most of the pions from hard Δ decay will be scattered in the evolution. Due to the scattering process, the Δ decay into free pions at freeze-out takes place in a wide density range. Nevertheless, the average density is up to $1.5\rho_0$. Therefore it is reasonable to use pion production to probe the properties of nuclear matter at high densities.

Figure 2 shows the evolution of the inelastic collision number in the reaction. As is commonly known, NN inelastic collisions and hard Δ decay take place in the early stage. The hard Δ mostly produces at the time of about 15 fm/c, and, after 30 fm/c, there is almost no new hard Δ production. It can also be estimated from Fig. 2 that the absorptivity of the pions is about 18%.

In the following, we focus on the charged pions at the freeze-out because of their advantage in the detector acceptance. With the analysis of the complex collision history, we classified the free charged pions according to the πN rescattering number in their history. Fractions of charged free pions originating from specific rescattering process are plotted in Fig. 3. Here the abscissa values are the cycle index of the πN

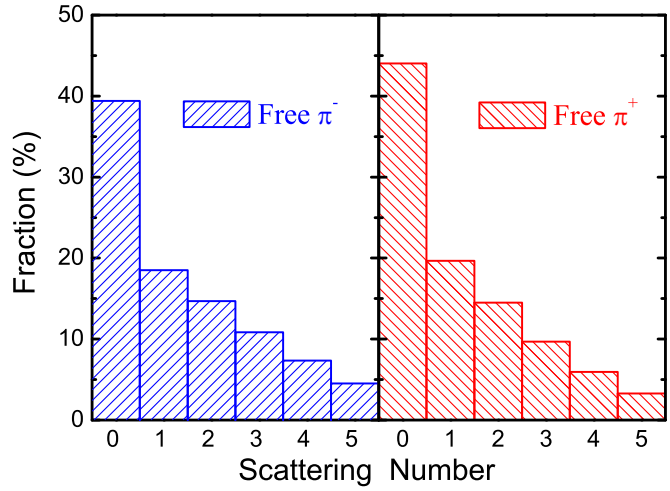

FIG. 3. Fraction of the different types of free pions categorized by their scattering numbers.

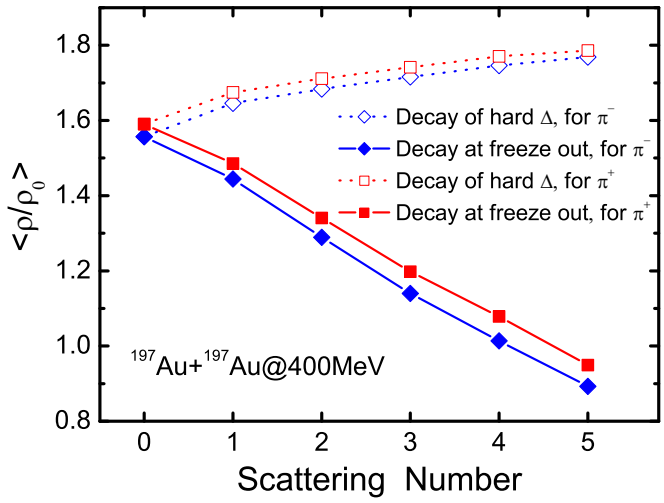

FIG. 4. The average density at which a pion was produced the first time by hard Δ decay (first pion formation) and a free pion was produced by the decay at freeze-out (last pion formation), versus the different types of free pions categorized by their scattering numbers.

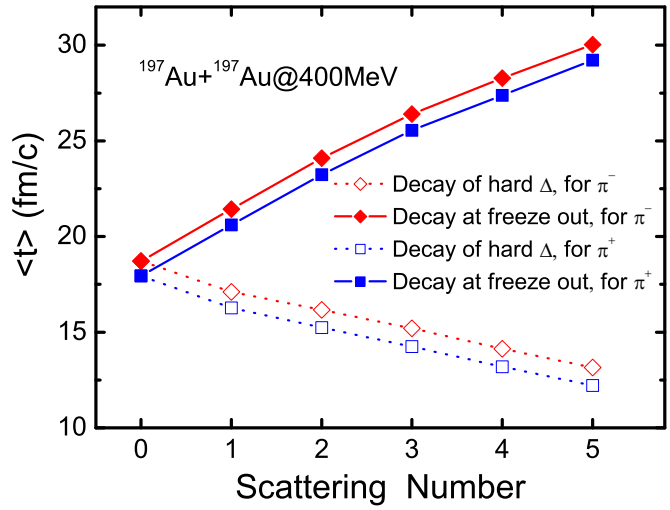

FIG. 5. The average time when a pion was produced the first time by hard Δ decay (first pion formation) and the decay at freeze-out (last pion formation), versus the different types of free pions categorized by their scattering numbers.

scattering of the collision history for the detectable pions. For example, 0 on the abscissa corresponds the pions without any absorption process after they are produced from hard Δ decay, 1 corresponds the pions having been πN scattered one time, i.e., by the channel $NN \to N\Delta \to NN\pi \to N\Delta \to NN\pi_{\text{free}}$, and so on.

It can been seen that most of the free pions have been absorbed into Δ and then redecay into pions after they are first produced by hard Δ decay. Our calculation shows less than 40% of the detectable negative pions are seen to freeze out as soon as they are produced by hard Δ decay, without any πN scattering. It can been also seen that at least 5% of the negative pions have been scattered at least five times before they are detected.

For positive pions, the fraction of those without a πN scattering process is about 44%, larger than that of the negative ones, as a result of the Coulomb potential from protons, i.e., negative pions are attracted while positive ones are repelled away.

We next investigate the pion creation history, and focus on the two processes. One is the first formation, i.e., the decay of the hard Δ into pions, another is last formation, i.e., the Δ decay into free pions at the freeze-out. Figure 4 shows the average density at which the first and last creations take place, for different categories of free pions which are categorized in Fig. 3. As shown, the average density of the first formation for all categories is apparently above the normal nuclear density. The pions with more scattering processes are mostly produced from hard Δ decay at higher density. The average density of the last formation of course is much lower than that of the first formation. Nevertheless, it is still above the normal nuclear density for most of th categories. The average densities of the formations of π^+ are a little higher than those of π^- because of the Coulomb potential.

Figure 5 shows the average time of the first and the last formations of the pion, versus the different categories of pion. One can see that for the categories of the pion with less scatterings, their first formations take place later. It is not surprising due to the fact that the pions which were created from Δ decay earlier have higher probabilities of being scattered, and the whole scattering process occurs in a larger time range.

Figure 6 shows the π^-/π^+ ratio for different categories of free pions, with soft and stiff symmetry energies. We can find that the ratios increase with increasing scattering number, in both situations. Because of the Coulomb potential, negative pions have higher probabilities of being absorbed and scattered than positive ones. It should also be noticed the effects of the symmetry energy are apparent for most categories. However, for the zero category, i.e., pions without any scattering process, the effects appear to be negligible.

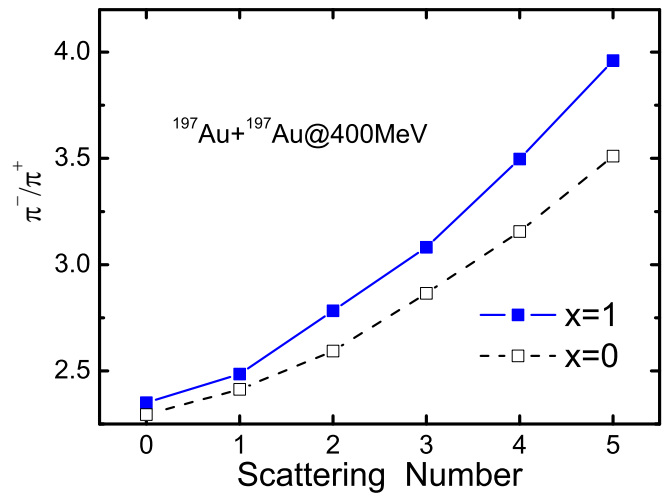

FIG. 6. The π^-/π^+ ratio versus the different types of free pions categorized by their scattering numbers in the central collision of Au + Au at a beam energy of 400 MeV/nucleon with different symmetry energies.

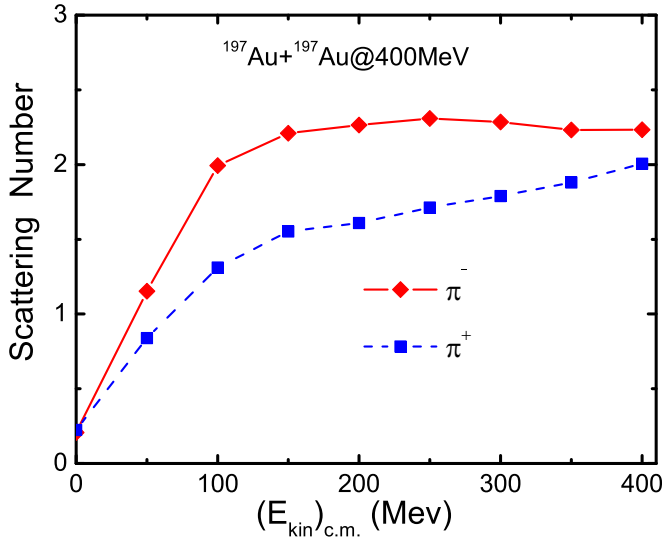

FIG. 7. The average scattering number in the history of the free pions as a function of the kinetic energy, in the central collision of Au + Au at a beam energy of 400 MeV/nucleon.

With increasing scattering number, the ratio shows more sensitivity to the symmetry energy. In particular, for the pions with five scattering processes, the effects reach to more than 15%. The difference of the sensitivity for different categories is reasonable. The pions without more scattering processes are created by hard Δ decay and freeze out to the detector directly. For those pions with more scattering processes, their first formations take place earlier and last formations take place later. Therefore, the time of their exit from high density matter is longer, which enhances the sensitivity to the stiffness of nuclear symmetry energy at high densities. This implies that the effect of the symmetry energy is governed not only by the density where the pions are originated but also by the time that they spent in the high density region during their whole formation processes.

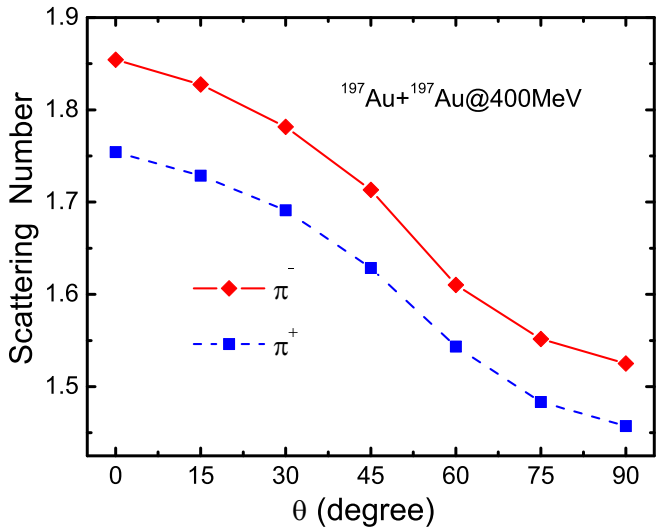

FIG. 8. The average scattering number in the history of the free pions as a function of the polar angle, in the central collision of Au + Au at a beam energy of 400 MeV/nucleon with different symmetry energies.

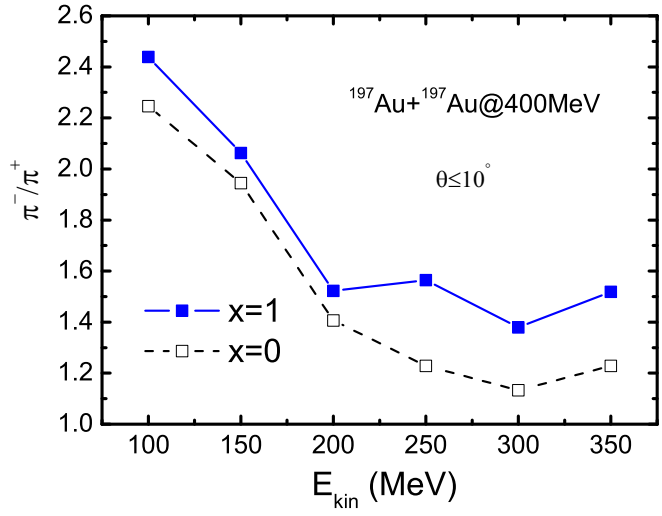

FIG. 9. Kinetic energy dependence of the ratios of the charged pions emitted in a direction closed to the beam direction at a beam energy of 400 MeV/nucleon with different symmetry energies.

It is difficult to differentiate between the pions with different scattering processes. We calculated the average scattering number, as shown in Fig. 7, as a function of kinetic energy. The results show the pions with higher kinetic energy mostly have more scattering processes. It should be noticed that in the kinetic energy spectrum at small $E_k \leqslant 50$ MeV the average scattering number is less than 1, indicating most of these pions have never been scattered since they were produced from hard Δ decay.

We also plot the azimuth dependence of the average scattering number in Fig. 8. Here θ is the polar angle of the emitted charged pions with respect to the z axis in the beam direction, i.e., $\theta = \arcsin(|p_t|/|p|)$. We can see that the pions emitted along the beam direction have more scattering processes.

Plotted in Fig. 9 is the kinetic energy dependence of the ratios of π^-/π^+ close to the beam direction. Since around the beam direction or at kinetic energies above 200 MeV pions have maximum scattering number, and the sensitivity of the charged pion ratio to the symmetry energy increases with the scattering numbers, it is thus not surprising to see that in this direction the free π^-/π^+ ratio at high kinetic energies ($E_{\rm kin} \geqslant 200$ MeV) exhibits significant sensitivity to the symmetry energy, and the effect can be more than 20%.

IV. CONCLUSIONS

In conclusion, based on the framework of the IBUU transport model, we investigated the central collision of Au + Au at a beam energy of 400 MeV/nucleon. We analyzed all the inelastic collisions to extract information on the pion production and its absorption. The statistical investigation shows that the pions are first produced by hard Δ decay at an average

density around $1.75\rho_0$. About 18% of them are absorbed absolutely in subsequent inelastic collisions, thus they cannot be observed in the experiment. From categorizing the free pions by their scattering processes, it is found that most of the free pions have been scattered one or more times, and the pions with higher scattering numbers carry more information on the high-density nuclear matter. Moreover, we investigate the azimuth dependence and the kinetic energy dependence of the scattering processes. The ratio of charged pions which are emitted a the direction close to the beam direction with high kinetic energies exhibits significant sensitivity to the symmetry energy.

ACKNOWLEDGMENTS

The work is supported by the National Natural Science Foundation of China (Grants No. 11875013, No. 11775275, No. 11975282, and No. 11705041) and the Scientific Research Program Funded by Shaanxi Provincial Education Department (Program No. 14JK1794).

[1] B. A. Li, L. W. Chen, and C. M. Ko, Phys. Rep. **464**, 113 (2008).
[2] V. Baran, M. Colonna, V. Greco, and M. Di Toro, Phys. Rep. **410**, 335 (2005).
[3] M. Colonna, Prog. Part. Nucl. Phys. **113**, 103775 (2020).
[4] S. Gautam, A. D. Sood, R. K. Puri, and J. Aichelin, Phys. Rev. C **83**, 034606 (2011).
[5] M. Di Toro, M. Colonna, V. Greco *et al.*, Int. J. Mod. Phys. E **17**, 1799 (2008).
[6] B. A. Li, G. C. Yong, and W. Zuo, Phys. Rev. C **71**, 014608 (2005).
[7] P. M. Lo, Phys. Rev. C **97**, 035210 (2018).
[8] M. D. Cozma, Phys. Rev. C **95**, 014601 (2017).
[9] Z. Zhang and C. M. Ko, Phys. Rev. C **95**, 064604 (2017).
[10] B. A. Li, Phys. Rev. C **92**, 034603 (2015).
[11] T. Song and C. M. Ko, Phys. Rev. C **91**, 014901 (2015).
[12] Y. Cui, Y. X. Zhang, and Z. X. Li, Phys. Rev. C **98**, 054605 (2018).
[13] M. Di Toro, V. Baran, M. Colonna *et al.*, Nucl. Phys. A **787**, 585 (2007).
[14] V. Prassa, G. Ferini, T. Gaitanos, H. H. Wolter, G. A. Lalazissis, and M. Di Toro, Nucl. Phys. A **789**, 311 (2007).
[15] M. D. Cozma, Phys. Lett. B **753**, 166 (2016).
[16] B. A. Li, Phys. Rev. Lett. **88**, 192701 (2002); Nucl. Phys. A **708**, 365 (2002).
[17] Q. F. Li, Z. Li, S. Soff, M. Bleicher, and H. Stöcker, J. Phys. G: Nucl. Part. Phys. **32**, 151 (2006).
[18] Y. Y. Liu, Y. J. Wang, Q. F. Li, and L. Liu, Phys. Rev. C **97**, 034602 (2018).
[19] Y. Gao, G. C. Yong, L. Zhang, and W. Zuo, Phys. Rev. C **97**, 014609 (2018).
[20] Y. Gao, G. C. Yong, Y. J. Wang, Q. F. Li, and W. Zuo, Phys. Rev. C **88**, 057601 (2013).
[21] Z. G. Xiao, B. A. Li, L. W. Chen, G. C. Yong, and M. Zhang, Phys. Rev. Lett. **102**, 062502 (2009).
[22] W. J. Xie, J. Su, L. Zhu, and F. S. Zhang, Phys. Lett. B **718**, 1510 (2013).
[23] Z. Q. Feng and G. M. Jin, Phys. Lett. B **683**, 140 (2010).
[24] H. H. Wolter, V. Prassa, G. Lalazissis, T. Gaitanos, G. Ferini, M. Di Toro, and V. Greco, Prog. Part. Nucl. Phys. **62**, 402 (2009).
[25] S. A. Bass, R. Mattiello, H. Stocker, and W. Greiner, Phys. Lett. B **302**, 381 (1993).
[26] B. A. Li, Nucl. Phys. A **570**, 797 (1994).
[27] M. Lv, Y. G. Ma, J. H. Chen, D. Q. Fang, and G. Q. Zhang, Phys. Rev. C **95**, 024614 (2017).
[28] B. A. Li and L. W. Chen, Phys. Rev. C **72**, 064611 (2005).
[29] E. E. Kolomeitsev *et al.*, J. Phys. G **31**, S741 (2005).
[30] B. A. Li, Phys. Rev. Lett. **85**, 4221 (2000).
[31] Z. Wang, C. Xu, Z. Z. Ren, and C. Gao, Phys. Rev. C **96**, 054603 (2017).
[32] Z. X. Yang, X. L. Shang, G. C. Yong, W. Zuo, and Y. Gao, Phys. Rev. C **100**, 054325 (2019).
[33] L. Zhang, Y. Gao, Y. Du *et al.*, Eur. Phys. J. A **48**, 30 (2012).
[34] C. B. Das, S. Das Gupta, C. Gale, and B. A. Li, Phys. Rev. C **67**, 034611 (2003).
[35] S. Huber and J. Aichelin, Nucl. Phys. A **573**, 587 (1994).
[36] A. Engel, W. Cassing, U. Mosel, M. Schafer, and Gy. Wolf, Nucl. Phys. A **572**, 657 (1994).
[37] B. J. VerWest and R. A. Arndt, Phys. Rev. C **25**, 1979 (1982).
[38] P. Danielewicz and G. F. Bertsch, Nucl. Phys. A **533**, 712 (1991).
[39] J. Cugnon, T. Mizutani, and J. Vandermeulen, Nucl. Phys. A **352**, 505 (1981).
[40] B. A. Li, A. T. Sustich, B. Zhang, and C. M. Ko, Int. J. Mod. Phys. E **10**, 267 (2001).
[41] G. F. Bertsch and S. Das Gupta, Phys. Rep. **160**, 189 (1988).
[42] G. C. Yong, Phys. Rev. C **96**, 044605 (2017).
[43] J. Aichelin, Phys. Rep. **202**, 233 (1991).
[44] G. C. Yong, B. A. Li, L. W. Chen, and W. Zuo, Phys. Rev. C **73**, 034603 (2006).
[45] Y. J. Wang, C. C. Guo, Q. F. Li *et al.*, Phys. Lett. B **778**, 207 (2018).
[46] Y. J. Wang, Q. F. Li, L. Yvonne *et al.*, Phys. Lett. B **802**, 135249 (2020).